

## ADVANCES IN LATTICE BOLTZMANN MODELING (LBM) TO SIMULATE TWO-PHASE DYNAMICS

Prashant K. Jain<sup>1</sup>, Rizwan-uddin<sup>2</sup>

University of Illinois at Urbana-Champaign  
Nuclear Plasma and Radiological Engineering  
104 S. Wright St., Urbana, IL, USA 61801  
[pkjain2@illinois.edu](mailto:pkjain2@illinois.edu)<sup>1</sup>, [rizwan@illinois.edu](mailto:rizwan@illinois.edu)<sup>2</sup>

### ABSTRACT

In this paper, a new lattice Boltzmann model, called the *artificial interface lattice Boltzmann model* (AILB model), is proposed for the simulation of two-phase dynamics. The model is based on the principle of free energy minimization and invokes the Gibbs-Duhem equation in the formulation of non-ideal forcing function. Bulk regions of the two phases are governed by a non-ideal equation of state (for example, the van der Waals equation of state), whereas an artificial near-critical equation of state is applied in the interfacial region. The interfacial equation of state is described by a double well density dependence of the free energy. The continuity of chemical potential is enforced at the interface boundaries. Using the AILB model, large density and viscosity ratios of the two phases can be simulated. The model is able to quantitatively capture the coexistence curve for the van der Waals equation of state for different temperatures. Moreover, spatially varying viscosities can be simulated by choosing the relaxation time as a function of local density.

### 1. INTRODUCTION

Dynamics of two-phase flows plays an important role in many fields of applied science and engineering, including oil-water flow in porous media, boiling fluids, liquid metal melting and solidification, and many more. Typically two-phase flows manifest a wide variety of geometrical patterns (or flow regimes) of associated phases depending on the system conditions. These patterns include, but are not limited to, bubbly, slug, churn and annular flows. These multiple flow patterns significantly affect the overall system hydrodynamics by varying the heat transfer and pressure drop characteristic of a given flow.

One specific example is a boiling water reactor (BWR) core, in which the coolant enters the core as liquid, undergoes a phase change as it traverses the core and exits as a high-quality two-phase mixture. Two-phase flows in BWRs typically manifest a wide variety of geometrical

patterns of the co-existing phases depending on the local thermodynamic conditions [1].

The accuracy in modeling is vital for the safety and economy of a nuclear power plant. However, modeling such flows—which involve bubble nucleation, bubble growth and coalescence, and inter-phase surface topology transitions—using CFD type approaches currently relies on empirical correlations and therefore, hinder the physics-based insightful predictions. For example, several best estimate codes in nuclear industry, such as RETINA, CATHRE still rely on the extrapolated results from some simple laboratory experiments. The empiricism in the closure relations is a major source of error in them.

To improve the accuracy, we must resolve the complexity of two-phase flow structures either by gathering information from the physical experiments (at similar system conditions) and/or from numerical/analytical methods. We should note that even now, the physics of very simple two-phase scenarios (for example, the growth of a single bubble on a heated surface and the coalescence of two bubbles) has not been fully understood. In an attempt to grasp the physics using state-of-the-art technologies, several experimental studies are currently being performed.

Several computational approaches, such as molecular dynamics, dissipative pseudo particle dynamics, direct simulation Monte Carlo and Navier-Stokes based approaches, are best suited at different time/space scales for fluid simulations. Cross-scale interactions (back-and-forth feeding of scale-specific solutions) are required at each level of scale hierarchy in order to gain better predictive modeling. This multi-scale strategy (merging results at the micro-, meso- and macro-scales) to simulate fluid flow may be able to better address the physics of complex fluids. However, advances should be first made in developing the scale-specific approach and strategies are required to merge the solutions at different scales in order to obtain reliable results [2-3]. Because of its mesoscopic nature, lattice Boltzmann (LBM) methodologies are a good fit in the realm of multi-scale simulations and can address problems

that involve multiple levels of physical and mathematical descriptions.

Unlike conventional numerical schemes based on the discretizations of macroscopic continuum equations, the LBM is a particle-based approach, in which collective behavior of particles is represented by a *single-particle probability distribution function*. Roots of LBM lie in the earlier lattice gas cellular automata (LGCA) models, in which, evolution of particles on a fixed lattice simulate the overall macroscopic behavior. The uniqueness of LBM stems from the fact that the macroscopic dynamics emerges from the simulation of very simple kinetic models that incorporate the essential physics of the microscopic (or mesoscopic) processes in the system. There underlies an *artificial micro-world* of particles ‘living’, ‘propagating’ and ‘colliding’ on a fixed lattice while conserving mass and momentum.

For hydrodynamic simulations, LBM models are much simpler and efficient to solve on a computer compared to solving its macro-counterpart partial differential equations (PDEs). Though LBM and its variations were proposed several decades ago, it is only with the recent advances in computing power that their applications to realistic problems are becoming a reality. This approach appears to be one of the most promising approaches due to its scalability with computing power and short as well as long term promises. Computing power will no doubt continue to increase; and hence the LBM is likely to be applicable to ever larger problems [4-7].

## 2. ARTIFICIAL INTERFACE (AILB) MODEL

A thermodynamically consistent lattice Boltzmann (LB) model for the two-phase simulations can be obtained if one treats the chemical potential as the driving force for the phase separation. Incorporation of the Gibbs-Duhem equation, which imposes constraints on thermodynamic variables of a given system at equilibrium, into the LB model can guarantee the recovery of the equilibrium phase-thermodynamics [8].

In this section, a new LB model, called the *artificial interface lattice Boltzmann* (AILB) model is proposed for the two-phase simulations. The model incorporates the Gibbs-Duhem equation in order to recover the equilibrium thermodynamics. In this model, a non ideal equation of state, such as the van der Waals equation of state (vdW EOS), is employed in the regions occupied by the bulk phases whereas an artificial equation of state is used in the interfacial region. The advantage of using an artificial equation of state in the interfacial regions is that the thickness of the interface can now be controlled in the two-phase simulations. Numerical experiments show that the

numerical stability is also enhanced if one chooses a thicker interface which allows simulation of large density and viscosity ratios. Moreover, it is proposed to choose a suitable scaling factor for the vdW EOS. After scaling down the vdW EOS, one can simulate larger density/viscosity ratios without even making the interface thicker.

### 2.1. Lattice Boltzmann equation (LBE)

The discrete Boltzmann (DB) equation in the presence of forcing  $\mathbf{F}$  can be written in the following form:

$$\frac{Df_a}{Dt} = \frac{\partial f_a}{\partial t} + \mathbf{v}_a \cdot \frac{\partial f_a}{\partial \mathbf{r}} = -\frac{f_a - f_a^{eq}}{\tau} + \frac{(\mathbf{v}_a - \mathbf{u}) \cdot \mathbf{F}}{\rho RT} f_a^{eq} \quad (1)$$

where  $f_a(\mathbf{r}, t)$  is a single-particle distribution function discretized in the microscopic velocity space,  $\mathbf{v}_a$  is the microscopic velocity of the fluid particles,  $\rho(\mathbf{r}, t)$  is the fluid density,  $\mathbf{u}(\mathbf{r}, t)$  is the fluid velocity,  $\tau$  is a relaxation time related to the kinematic fluid viscosity,  $R$  is the ideal gas constant,  $T$  is the temperature,  $\mathbf{F}$  is the force experienced by the fluid particles,  $\mathbf{r}$  is the position vector of the fluid particles and  $t$  is time.

In the DB equation,  $f_a^{eq}$  is a single-particle equilibrium distribution function which is derived from a Maxwell-Boltzmann distribution and can be approximated to [5]:

$$f_a^{eq} = w_a \left[ 1 + \frac{\mathbf{v}_a \cdot \mathbf{u}}{RT} + \frac{1}{2} \left( \frac{\mathbf{v}_a \cdot \mathbf{u}}{RT} \right)^2 - \frac{u^2}{2RT} \right] \quad (2)$$

where  $w_a (\equiv t_a \rho)$  are lattice constants which depend upon the chosen lattice type.

For a  $D_2Q_9$  lattice, shown in Figure 1(a), we have:

$$t_a = \begin{cases} 4/9 & a = 0 \\ 1/9 & a = 1, 2, 3, 4 \\ 1/36 & a = 5, 6, 7, 8 \end{cases} \quad (3)$$

For a  $D_3Q_{19}$  lattice, shown in Figure 1(b), we have:

$$t_a = \begin{cases} 1/3 & a = 0 \\ 1/18 & a = 1 \text{ to } 6 \\ 1/36 & a = 7 \text{ to } 18 \end{cases} \quad (4)$$

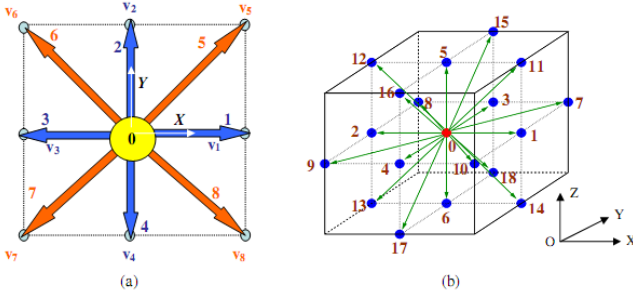


Figure 1. Lattice velocity directions in (a)  $D_2Q_9$  and (b)  $D_3Q_{19}$  lattice structures.

The DB equation is solved by employing a Lagrangian based discretization which essentially integrates it along the characteristics of the underlying lattice i.e.  $(\mathbf{r}, t) \rightarrow (\mathbf{r} + \mathbf{v}_a \Delta t, t + \Delta t)$ . In such an integration, steps in space and time are coupled with the microscopic velocity along the characteristics such that,  $\Delta \mathbf{r} = \mathbf{v}_a \Delta t$ . The resulting discretized equation is called the lattice Boltzmann (LB) equation, which is:

$$f_a(\mathbf{r} + \mathbf{v}_a \Delta t, t + \Delta t) - f_a(\mathbf{r}, t) = -\frac{\Delta t}{2\tau} \left[ f_a - f_a^{eq} \right] \Big|_{(\mathbf{r}, t)} - \frac{\Delta t}{2\tau} \left[ f_a - f_a^{eq} \right] \Big|_{(\mathbf{r} + \mathbf{v}_a \Delta t, t + \Delta t)} + \frac{\Delta t}{2} \frac{(\mathbf{v}_a - \mathbf{u}) \cdot \mathbf{F}}{\rho RT} f_a^{eq} \Big|_{(\mathbf{r}, t)} + \frac{\Delta t}{2} \frac{(\mathbf{v}_a - \mathbf{u}) \cdot \mathbf{F}}{\rho RT} f_a^{eq} \Big|_{(\mathbf{r} + \mathbf{v}_a \Delta t, t + \Delta t)} \quad (5)$$

## 2.2. Modified LBE

By defining the modified distribution function  $g_a(\mathbf{r}, t)$  as:

$$g_a(\mathbf{r}, t) = f_a(\mathbf{r}, t) + \frac{\Delta t}{2\tau} \left[ f_a - f_a^{eq} \right] \Big|_{(\mathbf{r}, t)} - \frac{\Delta t}{2} \frac{(\mathbf{v}_a - \mathbf{u}) \cdot \mathbf{F}}{\rho RT} f_a^{eq} \Big|_{(\mathbf{r}, t)} \quad (6)$$

the LB equation (5) can be transformed to the following form:

$$g_a(\mathbf{r} + \mathbf{v}_a \Delta t, t + \Delta t) = g_a(\mathbf{r}, t) - \frac{\Delta t}{\tau + 0.5\Delta t} \left[ g_a - f_a^{eq} \right] \Big|_{(\mathbf{r}, t)} + \frac{0.5\tau}{\tau + 0.5\Delta t} \frac{\Delta t (\mathbf{v}_a - \mathbf{u}) \cdot \mathbf{F}}{\rho RT} f_a^{eq} \Big|_{(\mathbf{r}, t)} \quad (7)$$

The modified distribution function  $g_a(\mathbf{r}, t)$  can be used to determine the macroscopic hydrodynamics using the following relations:

$$\rho(\mathbf{r}, t) = \sum_a f_a = \sum_a g_a \quad (8)$$

$$\mathbf{u}(\mathbf{r}, t) = \frac{1}{\rho} \left( \sum_a \mathbf{v}_a f_a \right) = \frac{1}{\rho} \left[ \left( \sum_a \mathbf{v}_a g_a \right) + \frac{\Delta t}{2} \mathbf{F} \right] \quad (9)$$

## 2.3. Forcing term to simulate phase segregation

The LB equation, with a constant forcing term (which can be zero) possesses an inherent ideal gas equation of state, and is not suitable for simulating the segregated phase dynamics encountered in scenarios involving two coexisting phases. In order to model the non-ideal behavior of phase segregation, inter-particle interactions have to be introduced into the forcing term of LB equation by accounting for the long range attractions  $\mathbf{F}_{attr}$  and short range repulsions  $\mathbf{F}_{rep}$  in addition to the constant body force  $\mathbf{F}_G$ . Adding those, we can define the net force  $\mathbf{F}$  as:

$$\mathbf{F} = \mathbf{F}_{attr} + \mathbf{F}_{rep} + \mathbf{F}_G \quad (10)$$

Adding the long range attractive forces  $\mathbf{F}_{attr}$ , the short range repulsive forces  $\mathbf{F}_{rep}$  and the constant body force  $\mathbf{F}_G$  (which usually is the standard gravitational force  $\rho g$ ), we can associate the net force  $\mathbf{F}$  to the thermodynamic pressure  $P_0$  as:

$$\mathbf{F} = -\nabla(P_0 - \rho RT) + \kappa \rho \nabla \nabla^2 \rho + \mathbf{F}_G \quad (11)$$

where  $P_0$  follows a non-ideal equation of state:

$$P_0 = \rho RT (1 + \tilde{b} \rho \chi) - \tilde{a} \rho^2 \quad (12)$$

## 2.4. Gibbs-Duhem equation

For two coexisting phases of a fluid to remain in equilibrium, both the mechanical as well as the chemical equilibrium must be established. This constraint can be satisfied by enforcing the Gibbs-Duhem equation for equilibrium, which states:

$$\nabla P_0 = \rho \nabla \mu_0 \quad (13)$$

where  $\mu_0$  is the bulk chemical potential which is defined as the first derivative of bulk free energy density  $E_0$  with respect to the fluid density. Combining equations (11) and (13), we get:

$$\mathbf{F} = \nabla(\rho RT) - \rho \nabla \mu + \mathbf{F}_G \quad (14)$$

where  $\mu = \mu_0 - \kappa \nabla^2 \rho$ .

### 2.5. Chemical potential $\mu_0$ in the AILB model

For the bulk liquid ( $\rho(x, y) \geq \rho_{liq}^{sat}$ ) and bulk vapor ( $\rho(x, y) \leq \rho_{vap}^{sat}$ ) regions, we can choose a non-ideal equation of state, such as the van der Waals equation of state (vdW EOS), which is [9]:

$$P_0^{bulk} = \frac{\rho RT_0}{1 - b\rho} - a\rho^2 \quad (15)$$

Bulk chemical potential  $\mu_0^{bulk}$  for the vdW EOS can be obtained from:

$$\mu_0^{bulk} = RT_0 \ln\left(\frac{\rho}{1 - b\rho}\right) + \frac{RT_0}{1 - b\rho} - 2a\rho \quad (16)$$

The interfacial free energy density  $E_0^{int}$  of a fluid can be modeled to take the following double well form [10]:

$$E_0^{int} = \beta(\rho - \rho_l^{sat})^2 (\rho - \rho_v^{sat})^2 \quad (17)$$

where  $\beta$  is a constant related to the surface tension of the fluid, and  $\rho_l^{sat}$  and  $\rho_v^{sat}$  are densities of the saturated liquid and vapor phases, respectively.

A relation between the interfacial chemical potential and the fluid density  $\rho$  can be derived as:

$$\mu_0^{int} = \frac{\partial E_0^{int}}{\partial \rho} = 4\beta(\rho - \rho_l^{sat})(\rho - \rho_v^{sat})(\rho - \rho_m^{sat}) \quad (18)$$

where  $\rho_m^{sat} = 0.5(\rho_l^{sat} + \rho_v^{sat})$  is the mean saturation density.

In order to ensure the continuity of the chemical potential at the interface boundaries, i.e. at  $\rho = \rho_{liq}^{sat}$  and  $\rho = \rho_{vap}^{sat}$ , the interfacial chemical potential  $\mu_0^{int}$  is shifted by the value of the bulk chemical potential at the interface boundary, i.e.

$$\mu_0^{bulk} \Big|_{\rho=\rho_l^{sat}} \text{ to give:}$$

$$\mu_0^{int} = \mu_0^{bulk} \Big|_{\rho=\rho_l^{sat}} + 4\beta(\rho - \rho_l^{sat})(\rho - \rho_v^{sat})(\rho - \rho_m^{sat}) \quad (19)$$

### 3. RESULTS AND DISCUSSIONS

A two-dimensional LBM simulation is performed using a D<sub>2</sub>Q<sub>9</sub> lattice, in which, two stationary (liquid) droplets, each of density 1, are initialized such that they are in thermodynamic equilibrium with the vapor phase of density 0.0025 (see Figure 2). A periodic box of size 600 x 1600 *lu* (lattice units) is chosen for the simulation. Both the droplets are assumed to be of the same radii equal to 200 *lu* and are

separated by a minimum spacing of 4 *lu*. Surface tension of fluid is specified as 0.005 (in LBM units). LBM relaxation times for both the liquid and vapor are taken as 0.001 and 0.5, respectively. The interface thickness in LBM formulation is taken as equal to 4 *lu* initially. The kinematic viscosity  $\nu$  of the liquid and vapor are related to their corresponding relaxation times  $\tau$  by  $\nu = \tau/3$ . The temporal evolution of the above specified system of two droplets is shown in Figure 2 (a) to (h).

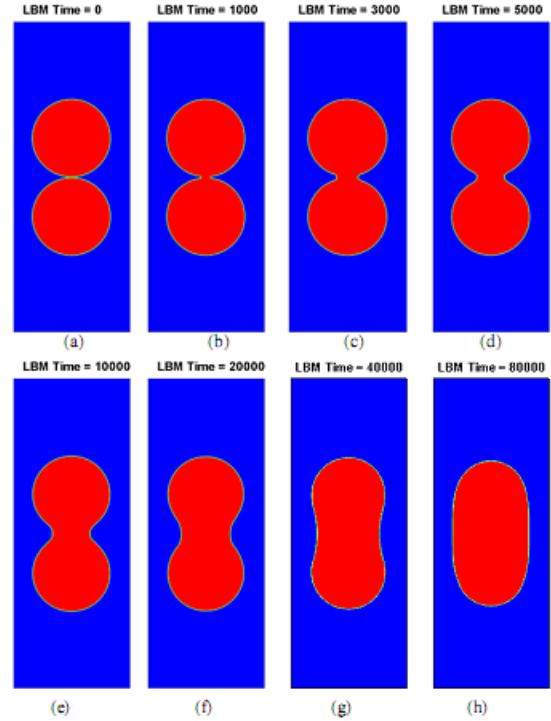


Figure 2. LBM simulation of coalescence of two stationary (liquid) droplets (see (a)). Due to the intermolecular attraction, a liquid bridge is initially formed between the two drops (see (b)) which then widens due to the presence of surface tension (see (c) to (h)) and later minimizes its surface energy by minimizing the perimeter of the liquid region to achieve the steady state in a shape of circular drop (not shown in figure). Other parameters of the simulations are:  $g = 0$ ,  $\rho_l = 1.0$  and  $\rho_v = 0.0025$ .

The radius of the liquid bridge  $r_b$  varies proportional to  $\propto \sqrt{t}$  and the corresponding variation in non-dimensional terms ( $r^* = \frac{r_b}{R_0}$ ,  $t^* = \frac{t}{\tau_i}$  and  $\tau_i = \sqrt{\frac{\rho_l R_0^3}{\sigma}}$ ) is shown in

Figure 3 for both, simulation results and experimental data for droplets of different radii. Reasonably good agreement between the two highlights the modeling capability and

applicability of the LBM for such simulations. It is intended that these validation studies will be followed by more complex LBM simulations of boiling phenomena relevant to BWRs in the future.

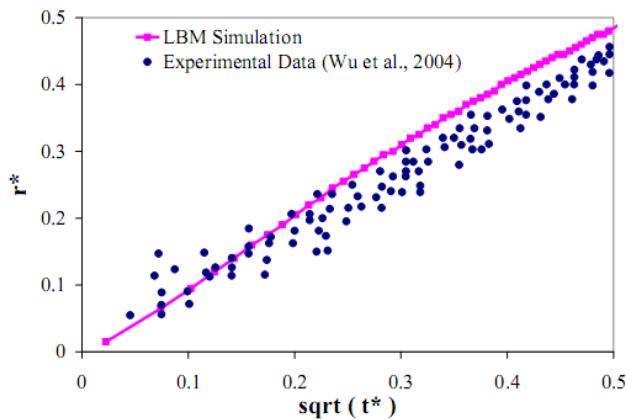


Figure 3. Variation of the non-dimensional bridge radius  $r^*$  with respect to the square-root of the non-dimensional inertial time  $\sqrt{t^*}$  for low viscosity fluids. Good agreement between the LBM simulation results (pink squares connected by a line) and experimental data for water drops of various radii (taken from [11]) is observed.

Several 2D LBM simulations of a single rising vapor bubble in a quiescent liquid have also been performed. The computational domain consists of  $200 \times 1000$  lattice points. No-slip LB boundary condition is specified on the bottom and top walls of the domain. Side boundaries are assumed to be periodic. A bubble of radius  $R = 50$  is initialized at  $t = 0$  to be of circular shape (in 2D) and located slightly above (about two bubble diameters) the bottom wall in order to reduce the possible wall-bubble interactions. Initially, both liquid and bubble are assumed to be stationary. Due to density difference between the vapor and the liquid phase and the presence of gravity, an upward buoyancy force acts on the lower-density bubble. The bubble moves upward and a liquid flow surrounding the bubble sets in due to the bubble's movement. This deforms the shape of the bubble from circular to 2D-oblate ellipsoidal. The deformation in bubble's shape is a natural consequence of the fluid flow fields (the wake below the lower surface and the recirculation on the sides).

The rising bubble is assumed to acquire a terminal shape when its area-averaged (in 2D) velocity attains a near-constant value, which for this simulation is found to be at nearly  $t = 70,000$  time steps. The terminal shape and the streamlines of flow around the bubble are shown in Figure 4 (a, b) in both the laboratory and the bubble's reference frame. The terminal shape from the LB simulations agrees well with the generalized shape regime map by Bhaga and

Weber [12] for the non-dimensional parameters of the simulation.

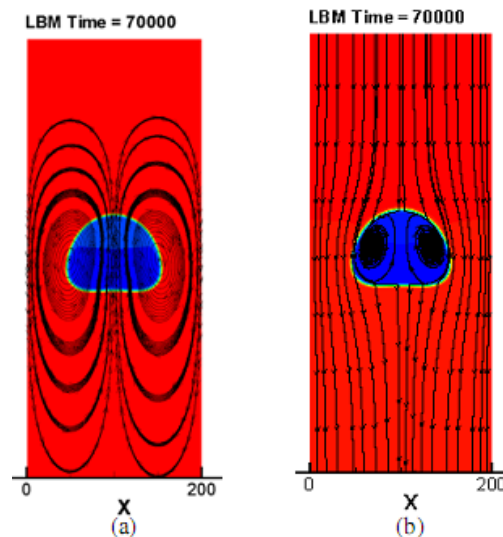


Figure 4. Terminal shape (oblate ellipsoidal) of a rising bubble and corresponding velocity stream lines after 70,000 LB time steps: (a) in the laboratory reference frame; and (b) in the bubble's reference frame. Parameters for the simulation are:  $\rho_l = 1.0$ ,  $\rho_v = 0.25$ ,  $R = 50$ ,  $\sigma = 5 \times 10^{-3}$ ,  $g = 10^{-5}$ ,  $\tau_l = \tau_v = 0.5$ ,  $L_x \times L_y = 200 \times 1000$ . (Red: liquid; blue: vapor.) Non-dimensional parameters are: Reynolds number,  $Re = 12.0$ ; Eotvos number,  $Eu = 15.0$  and Morton number,  $Mo = 0.046$ . Terminal velocity  $U_t$  is taken to be 0.02. The predicted shape agrees well with the corresponding shape in the regime map of Bhaga and Weber [12].

#### 4. CONCLUSIONS

An artificial interface lattice Boltzmann (AILB) model is proposed in this paper for the analysis of liquid-vapor two phase flows. Interface between the two fluid phases in the AILB model stretches across several grid points. Because of the diffuse interface description and the lattice Boltzmann evolution algorithm, moving interfaces are handled with a relative ease compared with the corresponding sharp-interface approaches. In the AILB algorithm, there is no need to explicitly track the phase-interface (i.e. to explicitly follow the position of the interfaces) or apply any interface conditions (such as, the continuity of shear stress etc.). Therefore, the overall computational complexity is reduced. The AILB model is able to handle singular topological events (such as, break-up and coalescence) without any need to introduce separate models for them. Simulation of such events in existing two-phase models usually requires special treatment in the solution algorithm. For example, in several other models, a

threshold on the thickness has to be prescribed in order to remove any thinning neck (or film) during the simulation of a break-up event. In the AILB model, no artificial trigger is needed to simulate bubble/drop breakup and coalescence. Due to the free-energy minimization principal of the AILB model, it could easily be extended to incorporate complex fluids (such as, polymers, colloids etc.). Several other interaction models could be included in composing the net free energy of the system, which upon minimization could produce desired interfacial events.

## 5. REFERENCES

- [1] Tong, L.S., Tang, Y.S., 1997. Boiling heat transfer and two-phase flow. Second edition, Taylor & Francis.
- [2] Yadigaroglu, G., 2005. Computational Fluid Dynamics for nuclear applications: from CFD to multi-scale CMFD. Nuclear Engineering and Design 235, 153-164.
- [3] Ninokata, H., 1999. Microscopic approaches in nuclear reactor thermal hydraulics computations. Ninth International Topical Meeting on Nuclear Reactor Thermal Hydraulics (NURETH-9), San Francisco, CA, October 3-8, 1999.
- [4] Succi, S., 2001. The Lattice Boltzmann Equation—for Fluid Dynamics and Beyond. Oxford Science Publications, UK.
- [5] Chen, S., Doolen, G.D., 1998. Lattice Boltzmann Method for Fluid Flows. Annu. Rev. Fluid Mech. 30, 329–364.
- [6] Lantermann, U., Hanel, D., 2007. Particle Monte Carlo and lattice-Boltzmann methods for simulations of gas-particle flows. Computers & Fluids 36, 407-422.
- [7] Rabbe, D., 2004. Overview of the lattice Boltzmann method for nano- and microscale fluid dynamics in materials science and engineering. Topical review in Modeling Simul. Mater. Sci. Eng. 12, R13-R46.
- [8] Wagner, A.J., 2006. Thermodynamic consistency of liquid-gas lattice Boltzmann simulations. Phys. Rev. E 74, 056703.
- [9] McQuarrie, D., Simon, J.D., 1999. Molecular Thermodynamics, University Science, Sausalito, CA.
- [10] Lee, T., Fischer, P.F., 2006. Eliminating parasitic currents in the lattice Boltzmann equation method for nonideal gases. Phys. Rev. E 74, 046709.
- [11] Wu, M., Cubaud, T., Ho, C.M., 2004. Scaling law in liquid drop coalescence driven by surface tension. Phys. Fluids 16, L51-L54.
- [12] Bhaga, D., Weber, M.E., 1981. Bubbles in viscous liquids: shapes, wakes and velocities. J. Fluid Mech. 105, 61-85.